INSTITUTE OF PLASMA PHYSICS

NAGOYA UNIVERSITY

Wave Propagation near the Lower Hybrid Resonance in Toroidal Plasmas

K. Ohkubo, K. Ohasa and K. Matsuura

IPPJ-233 Oct. 1975

RESEARCH REPORT

NAGOYA, JAPAN

Wave Propagation near the Lower Hybrid Resonance in Toroidal Plasmas

K. Ohkubo, K. Ohasa and K. Matsuura

IPPJ-233 Oct. 1975

Further communication about this report is to be sent to the Research Information Center, Institute of Plasma Physics, Nagoya University , Japan.

Abstract

Dielectric tensor and equipotential curves (ray trajectories) of an electrostatic wave near the lower hybrid resonance are investigated for the toroidal plasma with a shear magnetic field. The ray trajectories start from the vicinity of the plasma surface, and rotate in a spiral form around the magnetic axis, and then reach the lower or upper parts of lower hybrid resonance layer. The numerical computations are performed on the parameters of JIPP T-II device with two dimensional inhomogeneity.

§1. Introduction

Heating beyond the temperature initially achieved by an ohmic heating in low beta tokamak devices is a very important problem. Recently, the lower hybrid (LH) resonant heating has been considered as a leading method. The merit of the method originates in (i) the handling technique of the high power of the order of megawatts in the range of a few GHz, (ii) the launching method bought in large tokamak through waveguides, (iii) the possibility of heating electrons and ions to a deep region of the plasma.

There have been considerable interest, both theoretically and experimentally in the accessibility criterion[2-4] and the mode conversion[5,6] to the plasma wave near the resonant layer and impurity problem[8] in conection with the shift of the location of LH layer. If an electric field reaches the threshold for the parametric instability, the energy of the pump wave would be thermalized in the plasma. However, the efficiency of LH resonant heating and effects on transport phenomena are not made clear up to date. The dispersion relation of a wave at a frequency near the LH resonance in a hot plasma, which couples with ion cyclotron harmonic wave propagating obliquely to the magnetic field is complicated. But in a cold plasma theory, singularities and ray trajectories of the field of an electromagnetic wave in plasma with two-dimensional inhomogeneity in torus geometry are the interesting subjects. Recently, Javel et al.[11] studied experimentally the resonance cone-propagation properties and its wave structure in toroidal geometry (Wendelstein WIIa).

In this paper, the singularities and ray trajectories of the electromagnetic wave near LH frequency in JIPP T-II device[9] are studied taking into two dimensional inhomogeneity.

§2. Dielectric tensor

The singularities of the field of an electromagnetic wave in a cold plasma with two dimensional inhomogeneity have been studied by Piliya et al..[7,10] They showed that in the cartesian coordinates the characteristic was solved by a partial differential equation and the singularities were classified into the node and the saddle types.

A toroidally magnetized nonuniform plasma is assumed to be cold, while the plasma current I_p to be proportional to the electric conductivity which depends on the temperature. In order to analyze the electrostatic wave, which means the free-space wavelength is much larger than the wavelength in plasma, it is necessary to calculate the dielectric tensor in the presence of both toroidal, B_t, and poloidal magnetic field, B_p. The components of this tensor are calculated in cylindrical and cartesian coordinates. The latter is described in Appendix.

The equation of motion of a particle having mass m_s and charge e_s is given by

$$\frac{\partial \underline{V}_{s1}}{\partial t} + (\underline{V}_{s1}\cdot\nabla)\underline{V}_{s1} = \frac{e_s}{m_s}\,(\underline{E}_{s1} + \underline{V}_{s1}\times\underline{B}_t + \underline{V}_{s1}\times\underline{B}_p) \qquad (1)$$

The subscript 1 refers to the disturbances. B_p represents the poloidal field resulted from the plasma current I_p. When

the nonlinear term $(\underline{V}_{sl}\cdot\nabla)\underline{V}_{sl}$ is neglected and time dependence is assumed to be $e^{-j\omega t}$, the equation is written as

$$
\begin{aligned}
-j\omega V_{slr} &= (e_s/m_s)E_{slr} + V_{sl\theta}\omega_{cs} - V_{slz}\omega_{cs}A \ , \\
-j\omega V_{sl\theta} &= (e_s/m_s)E_{sl\theta} - V_{slr}\omega_{cs} \ , \\
-j\omega V_{slz} &= (e_s/m_s)E_{slz} + V_{slr}\omega_{cs}\,A \ ,
\end{aligned}
\tag{2}
$$

where ω_{cs} $(=e_sB_t/m_s)$ is the cyclotron frequency and $A = B_p/B_t$. Solving the each components of velocity we yield

$$
\begin{aligned}
V_{slr} &= -(e_s/m_s\Delta)(-\omega^2E_{slr} - j\omega\omega_{cs}E_{sl\theta} + j\omega\omega_{cs}AE_{slz}) \ , \\
V_{sl\theta} &= -(e_s/m_s\Delta)\{j\omega\omega_{cs}E_{slr} + (\omega^2A^2-\omega^2)E_{sl\theta} + \omega_{cs}^2AE_{slz}\} \ , \\
V_{slz} &= -(e_s/m_s\Delta)\{-j\omega\omega_{cs}AE_{slr} + \omega_{cs}^2AE_{sl\theta} + (\omega_{cs}^2-\omega^2)Eslz\} \ ,
\end{aligned}
\tag{3}
$$

where $\Delta = j\omega(\omega_{cs}^2 - \omega^2 + \omega_{cs}^2A^2)$.

By adding the convective current density $e_s\underline{V}_s N_s$ to the displacement current density in vacuum, we may define the dielectric tensor $\underline{\underline{\varepsilon}}$

$$
-j\omega\varepsilon_0\underline{\underline{\varepsilon}}\cdot\underline{E}_{sl} = e_s\underline{V}_{sl}N_s - j\omega\varepsilon_0\underline{E}_{sl} \tag{4}
$$

Using eqs.(3) and (4), we have

$$\underline{\underline{\varepsilon}} = \begin{pmatrix} 1 + \dfrac{\omega_{ps}^2}{Q} & \dfrac{j\omega_{ps}^2\omega_{cs}}{\omega Q} & -\dfrac{j\omega_{ps}^2\omega_{cs}A}{\omega Q} \\ -\dfrac{j\omega_{ps}^2\omega_{cs}}{\omega Q} & 1 - \dfrac{\omega_{ps}^2(\omega_{cs}^2A^2-\omega^2)}{\omega^2 Q} & -\dfrac{\omega_{ps}^2\omega_{cs}^2A}{\omega^2 Q} \\ \dfrac{j\omega_{ps}^2\omega_{cs}A}{\omega Q} & -\dfrac{\omega_{ps}^2\omega_{cs}^2A}{\omega^2 Q} & 1 - \dfrac{\omega_{ps}^2(\omega_{cs}^2-\omega^2)}{\omega^2 Q} \end{pmatrix}, \quad (5)$$

where $\omega_{ps}^2 = N_s e_s^2/m_s\varepsilon_0$ and $Q = \omega_{cs}^2 - \omega^2 + \omega_{cs}^2A^2$.

Here, $\underline{\underline{\varepsilon}}$ has the symmetry as $\varepsilon_{r\theta} = -\varepsilon_{\theta r}$, $\varepsilon_{\theta z} = \varepsilon_{z\theta}$ and $\varepsilon_{zr} = -\varepsilon_{rz}$, and is hermitian matrix. Although the poloidal magnetic field is smaller than toroidal one, the factor $(\omega_{cs}^2A^2-\omega^2)$, which is contained in $\varepsilon_{\theta\theta}$, plays an important role on the working frequency range.

§3. Characteristics and equipotential curves

In anisotropic plasma, perturbation from a localized rf source may propagate along a certain direction. Though, for simplicity, the cylindrical coordinates is used, the generalization to the pseudo-toroidal coordinates is straightforward. We use the divergence equation with the electrostatic approximation and assume that the plasma parameter is homogeneous along z-direction:

$$\nabla\cdot(\varepsilon_0\underline{\underline{\varepsilon}}\cdot\underline{E}) = 0$$
$$\underline{E} = -\nabla(\phi(r,\theta)e^{jk_{//}z}). \quad (6)$$

Substituting the dielectric tensor into eq.(6) the divergence equation becomes

$$\varepsilon_{rr}\frac{\partial^2\phi}{\partial r^2} + \frac{\varepsilon_{r\theta}+\varepsilon_{\theta r}}{r}\frac{\partial^2\phi}{\partial r\partial\theta} + \frac{\varepsilon_{\theta\theta}}{r^2}\frac{\partial^2\phi}{\partial\theta^2}$$
$$+ \frac{\partial\phi}{\partial r}\{\frac{\varepsilon_{rr}}{r} + \frac{\partial\varepsilon_{rr}}{\partial r} + \frac{1}{r}\frac{\partial\varepsilon_{\theta r}}{\partial\theta} + jk_{\prime\prime}(\varepsilon_{rz}+\varepsilon_{zr})\}$$
$$+ \frac{1}{r}\frac{\partial\phi}{\partial\theta}\{\frac{\partial\varepsilon_{r\theta}}{\partial r} + \frac{1}{r}\frac{\partial\varepsilon_{\theta\theta}}{\partial\theta} + jk_{\prime\prime}(\varepsilon_{z\theta}+\varepsilon_{\theta z})\} \qquad (7)$$
$$+ jk_{\prime\prime}\phi\ (\frac{\varepsilon_{rz}}{r} + \frac{\partial\varepsilon_{rz}}{\partial r} + \frac{1}{r}\frac{\partial\varepsilon_{\theta z}}{\partial\theta} + jk_{\prime\prime}\varepsilon_{zz}) = 0 \quad .$$

From eq.(7) we obtain the characteristics which coincide with equipotential curves <u>approximately</u>,

$$\varepsilon_{rr}(d\theta)^2 - \frac{\varepsilon_{r\theta}+\varepsilon_{\theta r}}{r}(dr)(d\theta) + \frac{\varepsilon_{\theta\theta}}{r^2}(dr)^2 = 0 \qquad (8)$$

Due to $\varepsilon_{r\theta} = -\varepsilon_{\theta r}$ in eq.(5) the above equation is reduced to

$$\frac{dr}{rd\theta} = \pm(-\varepsilon_{rr}/\varepsilon_{\theta\theta})^{1/2} \quad . \qquad (9)$$

Eq.(7) represents hyperbolic or elliptic type in accordance with the sign of $(-\varepsilon_{rr}/\varepsilon_{\theta\theta})$. In the periphery of plasma, eq. (7) is reduced to elliptic type and leads to an equipotential curves concentric about the localized source. The potential originated from the localized source decreases up to the hyperbolic-elliptic intersurface and then becomes constant along the characteristic in the hyperbolic region.

Because the intersurface of hyperbolic-elliptic region

is given by $\varepsilon_{\theta\theta} = 0$, it shows from eq.(9) that the characteristics are directed to the radial direction on its intersurface. While, on the hybrid resonance layer $\varepsilon_{rr} = 0$, the characteristics are parallel to the direction of poloidal field.

§4. Numerical analysis of the characteristics

In the numerical calculation of the characteristics, we used cartesian coordinates. The wave frequency in the vicinity of LH resonance is chosen as $\omega_{ci} << \omega << \omega_{ce}$. When there are impurities having mass M_j and concentration ratio C_j and charge $Z_j e$ in plasma, ion density n_i is equal to $n_e/(1+\Sigma C_j Z_j)$. Therefore, the characteristic equation (A3) in Appendix and the components of dielectric tensor are as follows:

$$\frac{dy}{dx} = - \frac{(S-G)\sin\gamma\cos\gamma \pm \sqrt{-SG}}{S\cos^2\gamma + G\sin^2\gamma} \quad , \tag{10}$$

where

$$G = S\cos^2\theta + P\sin^2\theta \ ,$$

$$S \simeq 1 + (\omega_{pe}^2/\omega_{ce}^2) - \frac{m_e}{M_i}\frac{\omega_{pe}^2}{\omega^2}\frac{1 + M_i\Sigma C_j Z_j^2/M_j}{1 + \Sigma C_j Z_j} \quad ,$$

$$P \simeq 1 - (\omega_{pe}^2/\omega^2) \quad .$$

This differential equation was solved numerically as functions of B_t, I_p, n_e, C_j and ω by Runge-Kutta-Gille method. Here, θ

is referred to the angle between z-axis and the composition of B_p and B_t, while γ is the angle between B_p and y-axis. That is

$$\sin\theta = B_p/(B_p^2 + B_t^2)^{1/2} \sim A \ ,$$

$$\tan\gamma = y/x \ ,$$

where an origin of x-and y-coordinates is the center of the plasma. The electron density $n_e(r)$, and the plasma current density $J(r)$, are assumed that

$$n_e(r) = n_e(0)(1 - r^2/a^2), \quad J(r) = J(0)(1 - r^2/a^2),$$

$$\text{and } r = (x^2 + y^2)^{1/2} \ ,$$

where a is the plasma radius, and $n_e(0)$, $J(0)$ are the values at the center of plasma. Therefore, B_p is written by

$$B_p(r) = \frac{\mu_0 I_p}{\pi a} \{(r/a) - (r/a)^3/2\} \ ,$$

while B_t is

$$B_t = R'B_0/(x + R) \ ,$$

where R' is the major radius of toroidal coils system, R is the major radius of the torus, and B_0 is the toroidal magnetic field strength at the center R'. Here, we ignored the vertical and the horizontal magnetic fields. The calculations are carried out by using the following parameters of JIPP T-II:[9)]

electron density, $n_e(0) \approx 10^{13}$ cm^{-3}

plasma radius, a = 17 cm

major radius of the torus, R = 91 cm

major radius of toroidal coils, $R' = 95$ cm

maximum toroidal magnetic field, $B_0 = 3.0$ wb/m^2.

The impurity in plasma is assumed to be oxygen having Z = 8. The initial points in Runge-Kutta-Gille-method were taken to be x(cm) = 15 cos(πn/6) and y(cm) = 15 sin(πn/6), where n = 0 $\sim$ 11 and the characteristics were computed inwards and outwards from the initial points.

For clarity, only one group of characteristics is shown in Figs.1-7. The others can be obtained easily by symmetric property with respect to x-axis. In figures the characteristics as the solid curve are plotted as a function of radial position r for the various plasma parameters. For reference, we also show the LH resonance layer as the dotted curve. At the constant frequency of 805 MHz, the plasma parameters are given in figures, where N is the peak density, J the plasma current, BT the toroidal magnetic field and IM the concentration of impurity. As shown in Figs.1-3, when the electron density increases to a certain value LH resonant layer appears and then enlarges to the outer region. Firstly, the characteristic starts in the radial direction from the vicinity of the periphery, and rotates in a spiral form several times around the magnetic axis and tends to be parallel to the poloidal field, and finally reaches LH resonant layer. In Fig.2 there are some characteristics which terminate in the center of plasma without access to the LH layer. Even $k_{\parallel} = 0$,

which can not satisfy the accessibility criterion[4] $N_{\parallel}^2 > 1 + \omega_{pe}^2/\omega_{ce}^2$, the waves would be propagated into the plasma core in the presence of an accessibility condition for poloidal direction. Since the electric field is given by $-\nabla\phi$, rf electric field in the weaker toroidal field of outer side of torus is larger than that in the region of the stronger field of inner side as shown in Figs.2 - 6. With increasing the electron density the traces of characteristics and LH layer shift slightly outwards. It is seen that on the LH resonant layer all the characteristics which start at the intersurface of hyperbolic-elliptic region do not terminate uniformly in space but concentrate at the lower (or upper) part on LH layer. If we assume that a plasma is homogeneous and the toroidal and poloidal magnetic fields are uniform and $k_{\parallel} = 0$, then the longitudinal dielectric constant $\varepsilon_\ell (= \underline{k}_\perp \cdot \underline{\underline{\varepsilon}} \cdot \underline{k}_\perp)$ is equal to $\varepsilon_{xx}k_x^2 + (\varepsilon_{xy}+\varepsilon_{yx})k_x k_y + \varepsilon_{yy}k_y^2$ and is zero from the dispersion relation. By using the group velocity in electrostatic approximation, which is given by $\underline{V_g} = -(\partial\varepsilon_\ell/\partial\underline{k}_\perp)_{\varepsilon_\ell=o}/(\partial\varepsilon_\ell/\partial\omega)_{\varepsilon_\ell=o}$ we obtain the ratio $V_{gx}/V_{gy} = -V_{phy}/V_{phx}$. Then, the group velocity is perpendicular to the phase velocity. Since this electrostatic wave is backward, the phase velocity which is parallel to the rf electric field travels outwards. Therefore the energy of the wave flows along the characteristic. In most calculations the safety factor q of the plasma current is taken to be 1.91 at surface. When the plasma current decreases by two times as shown in Figs.6 and 7, the beginning of characteristic displaces inwards and the curves reach rapidly LH resonant layer. As shown in Fig.8 it is observed that the location of the LH

resonant layer moves inwards with increasing impurities, until LH resonant layer disappears.

§5. Discussion and Conclusion

In a toroidal plasma with shear magnetic field, a dielectric tensor is calculated and the characteristic of the field of an electromagnetic wave in cold toroidal plasma is discussed and computed numerically. The characteristic begins towards the radial direction at $\varepsilon_{\theta\theta} = 0$ and rotates in a spiral form around the center of plasma, and reaches lower or upper parts on LH resonant layer along the poloidal magnetic field. It is found that the electric fields in a region of weaker toroidal field become rather higher than that in stronger region. It is confirmed that when the plasma current decreases, the beginning of characteristic shifts inwards and the curves reach rapidly LH resonant layer. We also examined the effect of impurity of fully ionized oxygen contained in plasma. Even if percentages of impurity is small the location of LH resonant layer and characteristics are sufficiently changed.

Arkhipenko et al.[10] showed that the maximum absorption of wave occurred at the region of weaker toroidal magnetic field and the node point was created there. In our case, however, the terminal points concentrate at the lower or upper parts of LH layer. Not only at these singularities but also at the stronger electric field near the region of weaker toroidal field, the transformation of electromagnetic waves into plasma waves will occur. In a hot plasma, the above electrostatic wave is converted into the plasma wave which

propagates outwards. At the turning point[12] which depends strongly on T_i and $N_{\parallel}$, but slightly on T_e, the heating of plasma is expected. Therefore, the turning points are shifted outwards from location of the singularities expected in cold plasma theory and attractive heating zone shapes the concentric form by the presence of the magnetic surface. Finally, we emphasized that when there may be accessibility condition for poloidal direction, the electromagnetic waves enter to the plasma core even if $k_{\parallel} = 0$.

The calculations of this work were made by HITAC 8500 computer of Institute of Plasma Physics, Nagoya University.

Appendix

The dielectric tensor in coordinates (x', y', z'), where the magnetic field is applied along z-axis is well known as

$$\underline{\underline{\varepsilon}}' = \begin{pmatrix} S & -jD & 0 \\ jD & S & 0 \\ 0 & 0 & P \end{pmatrix},$$

where S, D, P are given in ref.2. Firstly, the transformation of coordinates is performed by rotating around x'-axis by the angle of θ, and then the dielectric tensor in coordinates (x', y", z) can be obtained. Secondly, the same transformation is carried out by rotating around z-axis by the angle of γ.

$$\underline{\underline{\varepsilon}} = \underline{\underline{U}}_1 \cdot (\underline{\underline{U}}_0 \cdot \underline{\underline{\varepsilon}}' \cdot \underline{\underline{U}}_0^{-1}) \cdot \underline{\underline{U}}_1^{-1}$$

where

$$\underline{\underline{U}}_0 = \begin{pmatrix} 1 & 0 & 0 \\ 0 & \cos\theta & \sin\theta \\ 0 & -\sin\theta & \cos\theta \end{pmatrix}, \qquad \underline{\underline{U}}_1 = \begin{pmatrix} \cos\gamma & \sin\gamma & 0 \\ -\sin\gamma & \cos\gamma & 0 \\ 0 & 0 & 1 \end{pmatrix},$$

$$\underline{\underline{U}}_0 \cdot \underline{\underline{U}}_0^{-1} = 1 \quad \text{and} \quad \underline{\underline{U}}_1 \cdot \underline{\underline{U}}_1^{-1} = 1 .$$

The dielectric components are as follows:

$$\begin{aligned} \varepsilon_{xx} &= S\cos^2\gamma + G\sin^2\gamma , \\ \varepsilon_{xy} &= -S\sin\gamma\cos\gamma - jD\cos\theta + G\sin\gamma\cos\gamma , \\ \varepsilon_{xz} &= jD\sin\theta\cos\gamma + (P-S)\sin\theta\cos\theta\sin\gamma , \\ \varepsilon_{yx} &= -S\sin\gamma\cos\gamma + jD\cos\theta + G\sin\gamma\cos\gamma , \end{aligned}$$

$$
\left.
\begin{aligned}
\varepsilon_{yy} &= S\sin^2\gamma + G\cos^2\gamma \ , \\
\varepsilon_{yz} &= -jD\sin\theta\sin\gamma + (P-S)\sin\theta\cos\theta\cos\gamma \ , \\
\varepsilon_{zx} &= -jD\sin\theta\sin\gamma + (P-S)\sin\theta\cos\theta\cos\gamma \ , \\
\varepsilon_{zy} &= jD\sin\theta\sin\gamma + (P-S)\sin\theta\cos\theta\cos\gamma \ , \\
\varepsilon_{zz} &= S\sin^2\theta + P\cos^2\theta \ ,
\end{aligned}
\right\} \qquad \text{(A1)}
$$

where $G = S\cos^2\theta + P\sin^2\theta$.

The divergence equation

$$
\begin{aligned}
&\nabla\cdot(\varepsilon_0 \underline{\underline{\varepsilon}}\cdot\underline{E}) = 0, \\
&\underline{E} = -\nabla(\phi(x,y)e^{jk_{''}z}) \ ,
\end{aligned}
$$

is reduced to

$$
\begin{aligned}
&\varepsilon_{xx}\frac{\partial^2\phi}{\partial x^2} + (\varepsilon_{xy}+\varepsilon_{yx})\frac{\partial^2\phi}{\partial x\partial y} + \varepsilon_{yy}\frac{\partial^2\phi}{\partial y^2} \\
&+ \frac{\partial\phi}{\partial x}\{\frac{\partial\varepsilon_{xx}}{\partial x} + \frac{\partial\varepsilon_{yx}}{\partial y} + jk_{''}(\varepsilon_{xz}+\varepsilon_{zx})\} \\
&+ \frac{\partial\phi}{\partial y}\{\frac{\partial\varepsilon_{xy}}{\partial x} + \frac{\partial\varepsilon_{yy}}{\partial y} + jk_{''}(\varepsilon_{yz}+\varepsilon_{zy})\} \\
&+ jk_{''}\phi(\frac{\partial\varepsilon_{xz}}{\partial x} + \frac{\partial\varepsilon_{yz}}{\partial y} + jk_{''}\varepsilon_{zz}) = 0 \ .
\end{aligned} \qquad \text{(A2)}
$$

From eq.(A2) the characteristics[7] are determined by

$$
\frac{dy}{dx} = -\frac{-\sigma \pm \sqrt{\sigma^2 - \varepsilon_{xx}\varepsilon_{yy}}}{\varepsilon_{xx}}
$$

where

$$
\sigma=(\varepsilon_{xy}+\varepsilon_{yx})/2 = -S\sin\gamma\cos\gamma + G\sin\gamma\cos\gamma \ .
$$

Substituting the dielectric constant (A1), we have

$$\frac{dy}{dx} = - \frac{(S-G)\sin\gamma\cos\gamma \pm \sqrt{-SG}}{S\cos^2\gamma + G\sin^2\gamma} \qquad \text{(A3)}$$

References

1) T. H. Stix: MATT-1089 (Plasma Phys. Lab., Princeton Univ. 1974, Symposium on Plasma Heating in Toroidal Devices, Varenna, Italy, 1974).

2) T. H. Stix: Theory of Plasma Waves (McGraw Hill, New York, 1962).

3) P. Bellan and M. Porkolab: Phys. Rev. Letters 34, 124 (1975).

4) V. E. Golant: Zh. Tekh. Fiz. 41, 2492 (1971); Sov. Phys. Tech. Phys. 16, 1980 (1972).

5) T. H. Stix: Phys. Rev. Letters 15, 878 (1965).

6) A. Piliya and V. L. Fedorov: Zh. Eksp. Teor. Fiz. 57, 1198 (1969); Sov. Phys. JETP 30 653 (1970).

7) A. Piliya and V. L. Fedorov: Zh. Eksp. Teor. Fiz. 60, 389 (1971); Sov. Phys. JETP 33, 210 (1971).

8) A. H. Kritz and O. Eldridge: Nuclear Fusion 15, 465 (1975).

9) Project JIPP-II, IPPJ-205 (Inst. Plasma Phys., Nagoya Univ., Nagoya, Japan 1974).

10) V. I. Arkhipenko, A. B. Berezin, V. N. Budnikov, V. E. Golant, K. M. Novik, A. A. Obukov, A. D. Piliya, V. I. Fedorov, K. G. Shakhovets: Proceedings of the Fourth Conference on Plasma Physics and Controlled Nuclear Fusion Research, IAEA, Madison (1971), CN28/L-4.

11) P. Javel, G. Müller, U. Weber and R. R. Weynants: IPP2/228 (Max-Planck-Institut für Plasmaphysik, 1975).

12) K. Ohkubo and K. Matsuura: Annual Rev., Inst. of Plasma

Phys., Nagoya Univ., Nagoya, Japan, Apr. 1974 - Mar. 1975).

Figure Captions

Fig.1 The characteristics of electrostatic wave near the LH resonance. For clarity, only one family of the characteristics is drawn. The center of major radius is at the left side of the circle that is the plasma-vacuum boundary. In this figure there is no LH resonance layer.

Fig.2 The characteristics of electrostatic wave near the LH resonance. The characteristics started from A, B and C are not attain to LH layer but to the center of plasma. LH layer is drawn as the dotted curve.

Fig.3 The characteristics of electrostatic wave near the LH resonance. All the characteristics started from the outer region can not reach the LH layer in the region of the weaker toroidal magnetic field.

Fig.4 The characteristics of electrostatic wave near the LH resonance. In comparison with Figs.1-3, the toroidal field and the plasma current are increased by two times. LH layer becomes circle-like.

Fig.5 The characteristics of electrostatic wave near the LH resonance.

Fig.6 The characteristics of electrostatic wave near the LH resonance. The electron density is increased in comparison with that in Fig.5.

Fig.7 The characteristics of electrostatic wave for smaller plasma current (larger safety factor) than that in Fig.6.

Fig.8 The characteristics of electrostatic wave in a plasma with impurity of O^{+8}. The other parameters are the same as one in Fig.5.

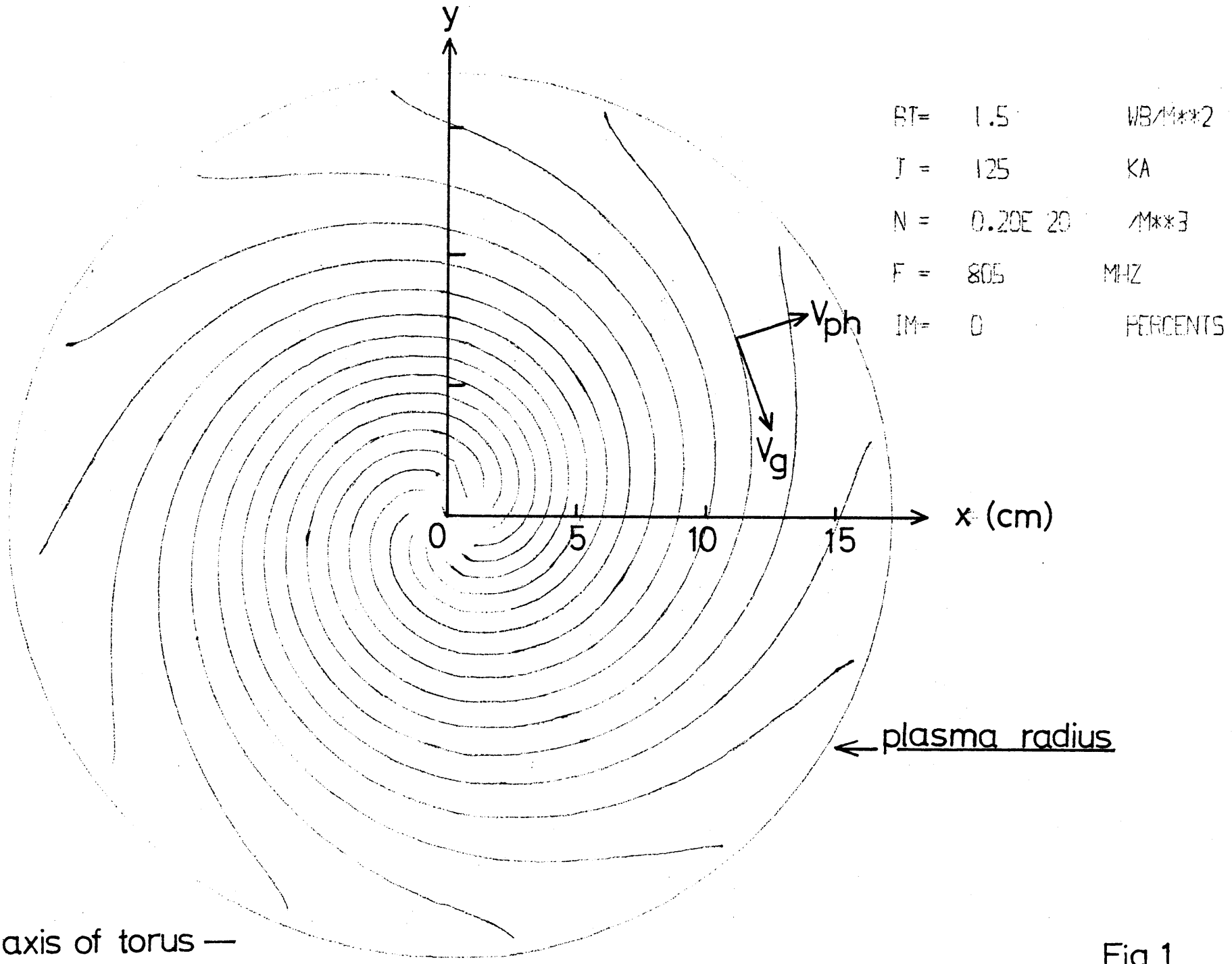
y
x (cm)
0
5
10
15
V_{ph}
V_g
BT= 1.5 WB/M**2
J = 125 KA
N = 0.20E 20 /M**3
F = 805 MHZ
IM= 0 PERCENTS
plasma radius
axis of torus

Fig. 1

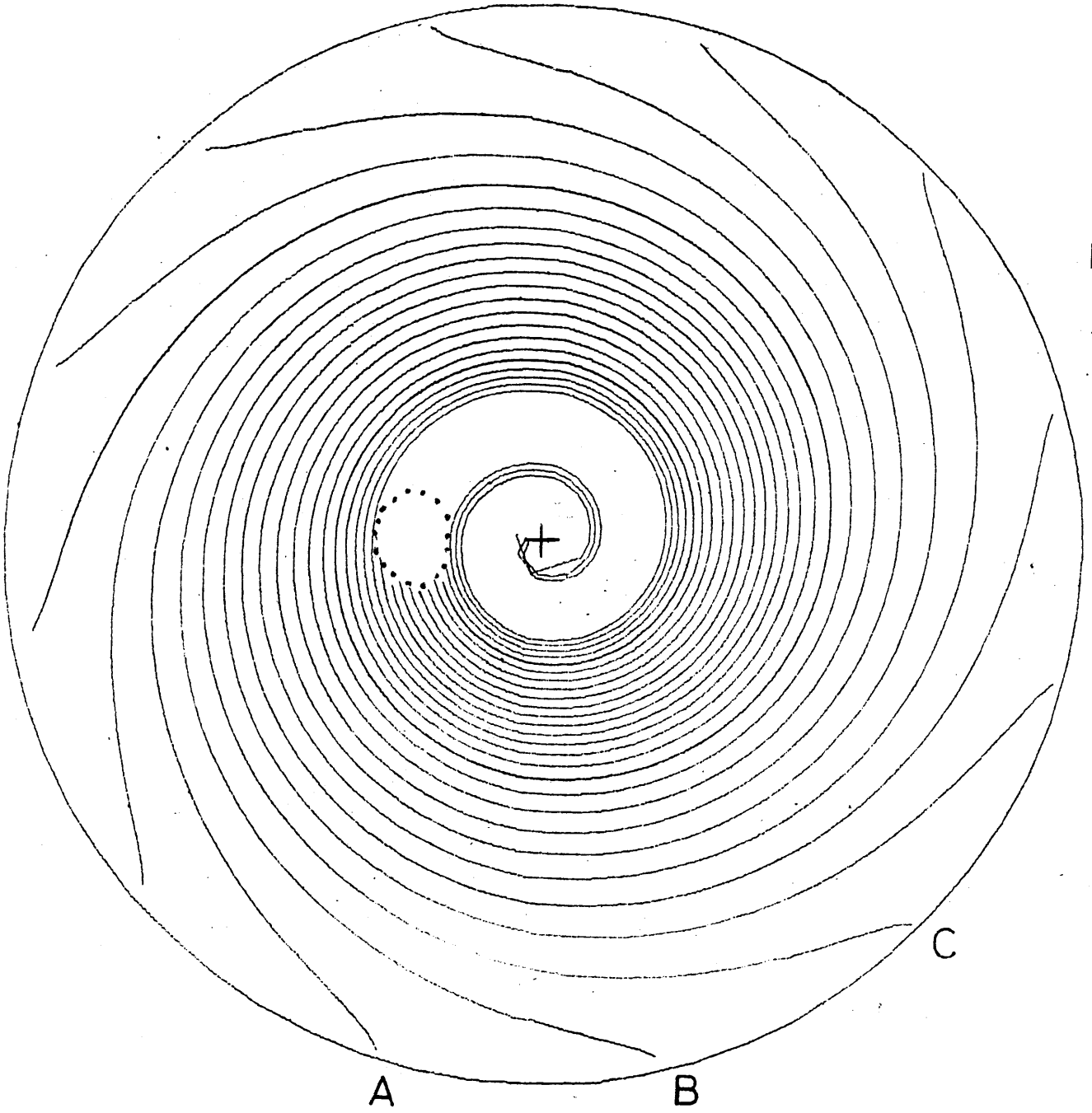

BT= 1.5 WB/M**2

J = 125 KA

N = 0.362E 20 /M**3

F = 805 MHZ

IM= 0 PERCENTS

Fig. 2

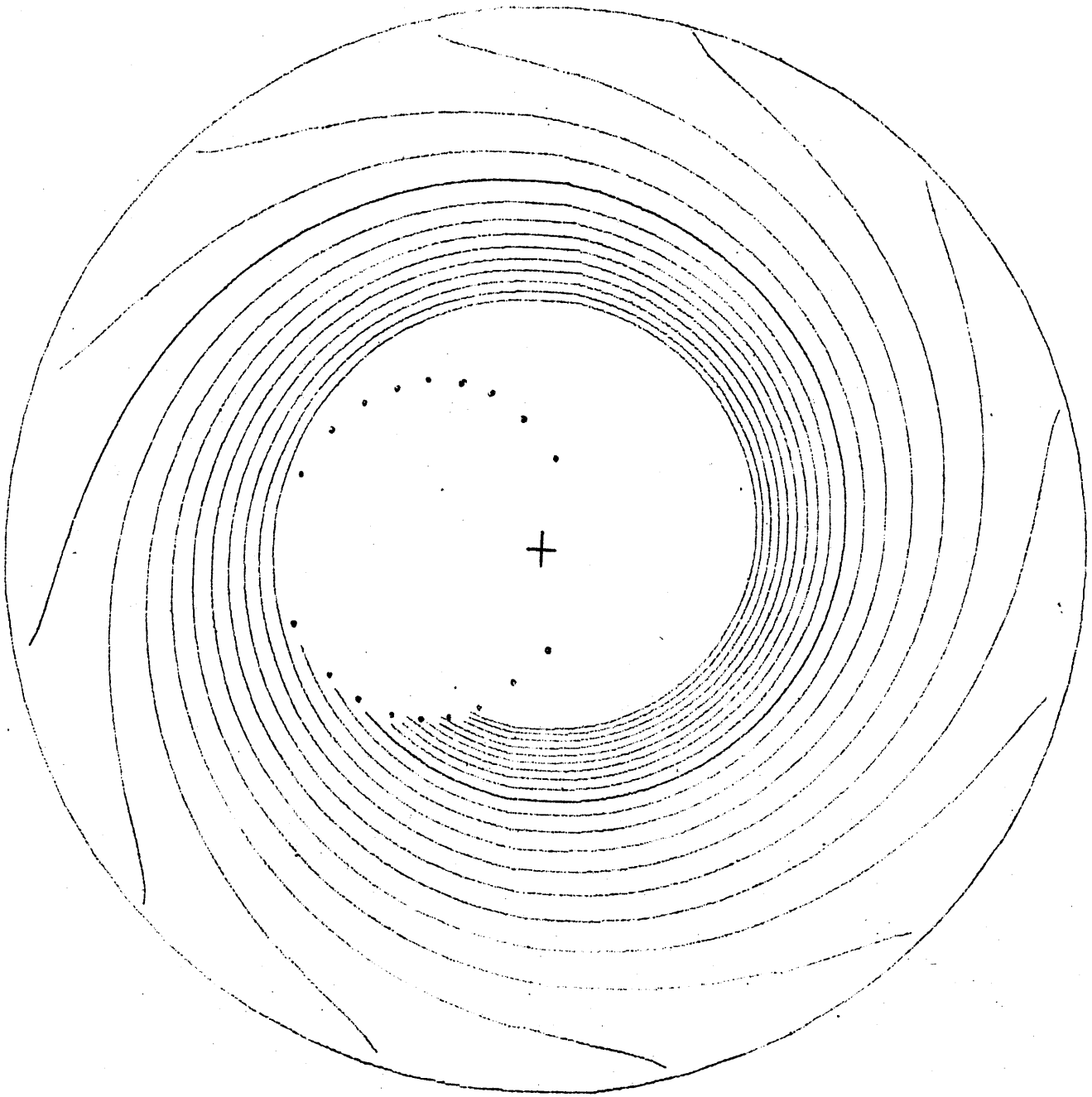

BT= 1.5 WB/M**2

J = 125 KA

N = 0.40E 20 /M**3

F = 805 MHZ

IM= 0 PERCENTS

Fig. 3

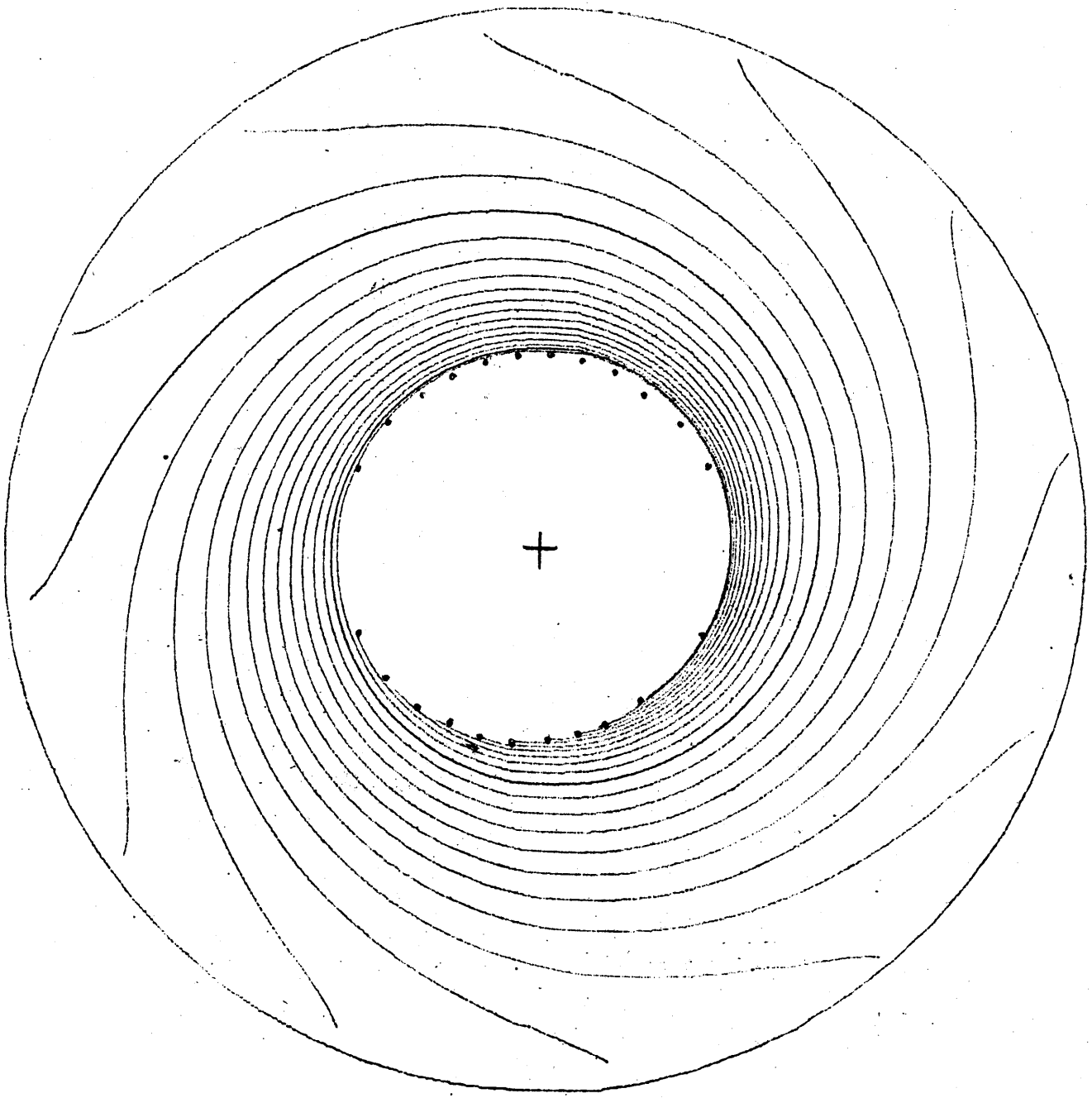

BT= 3.0 WB/Mkk2

J = 250 KA

N = 0.20E 20 /Mkk3

F = 805 MHZ

IM= 0 PERCENTS

Fig.4

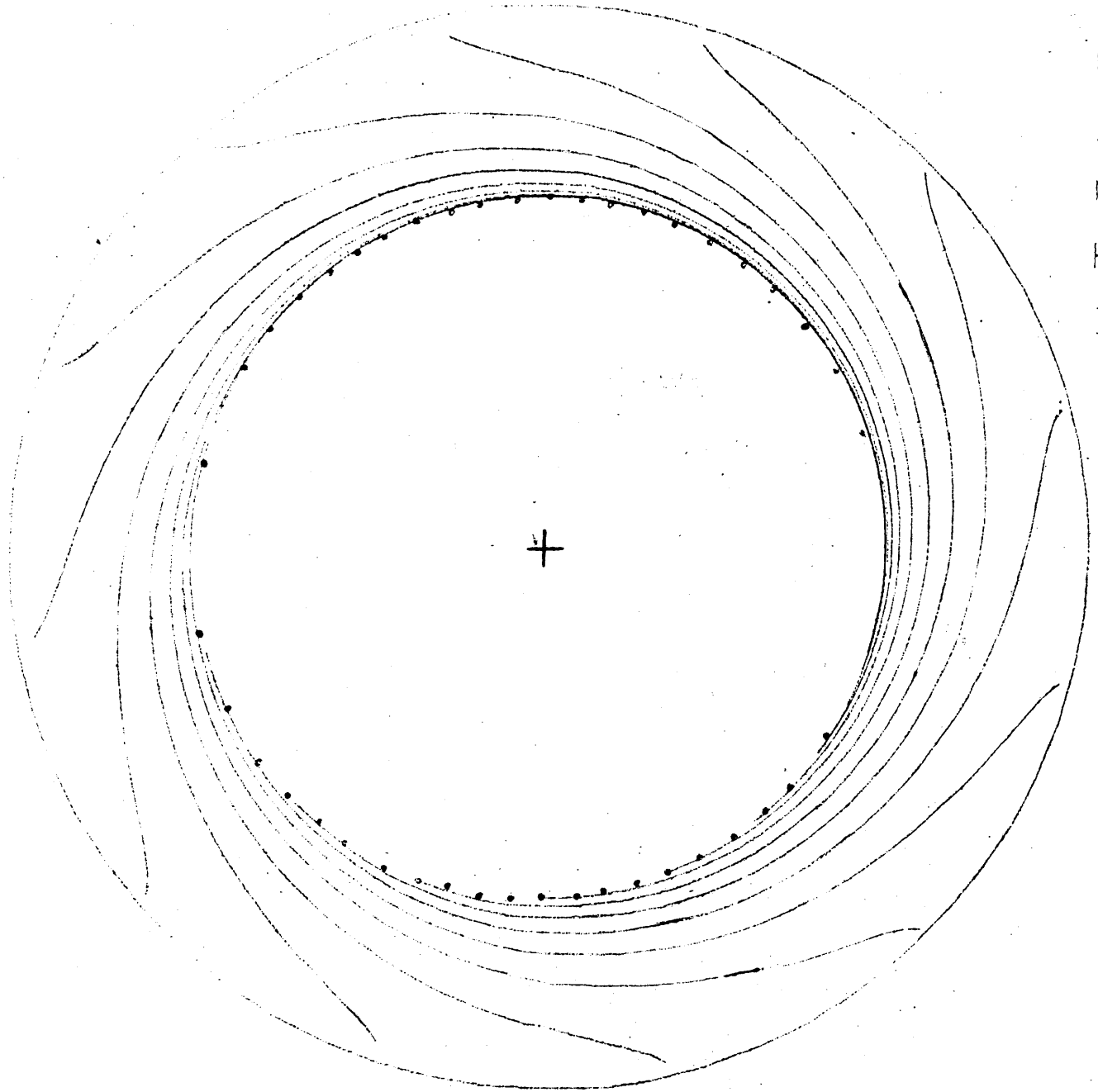

BT= 3.0 WB/M**2

J = 250 KA

N = 0.30E 20 /M**3

F = 805 MHZ

IM= 0 PERCENTS

Fig. 5

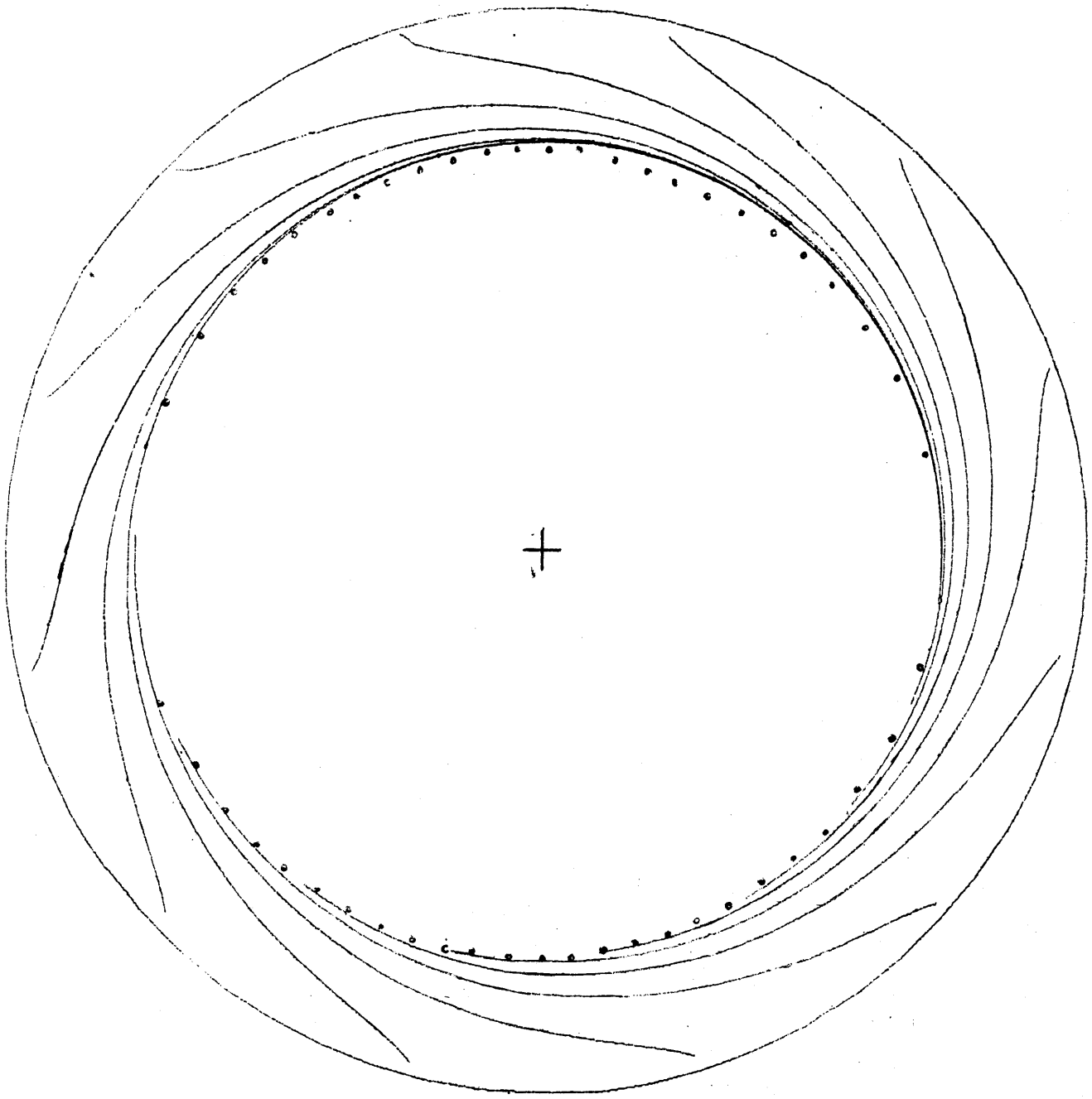

BT= 3.0 WB/M**2

J = 250 KA

N = 0.40E 20 /M**3

F = 805 MHZ

IM= 0 PERCENTS

Fig.6

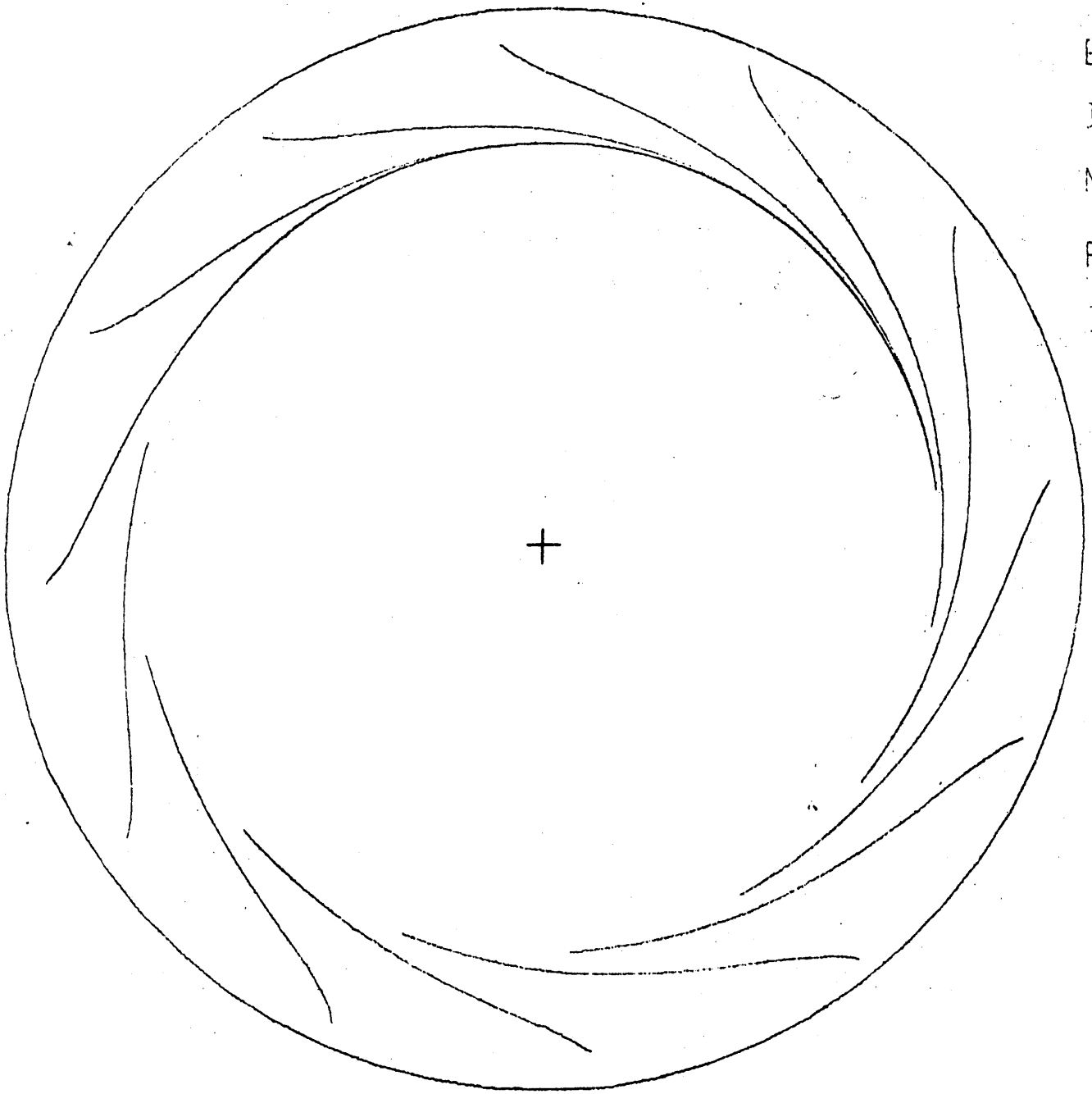

BT= 3.0 WB/M**2

I = 125 KA

N = 0.40E 20 /M**3

F = 805 MHZ

IM= 0 PERCENTS

Fig.7

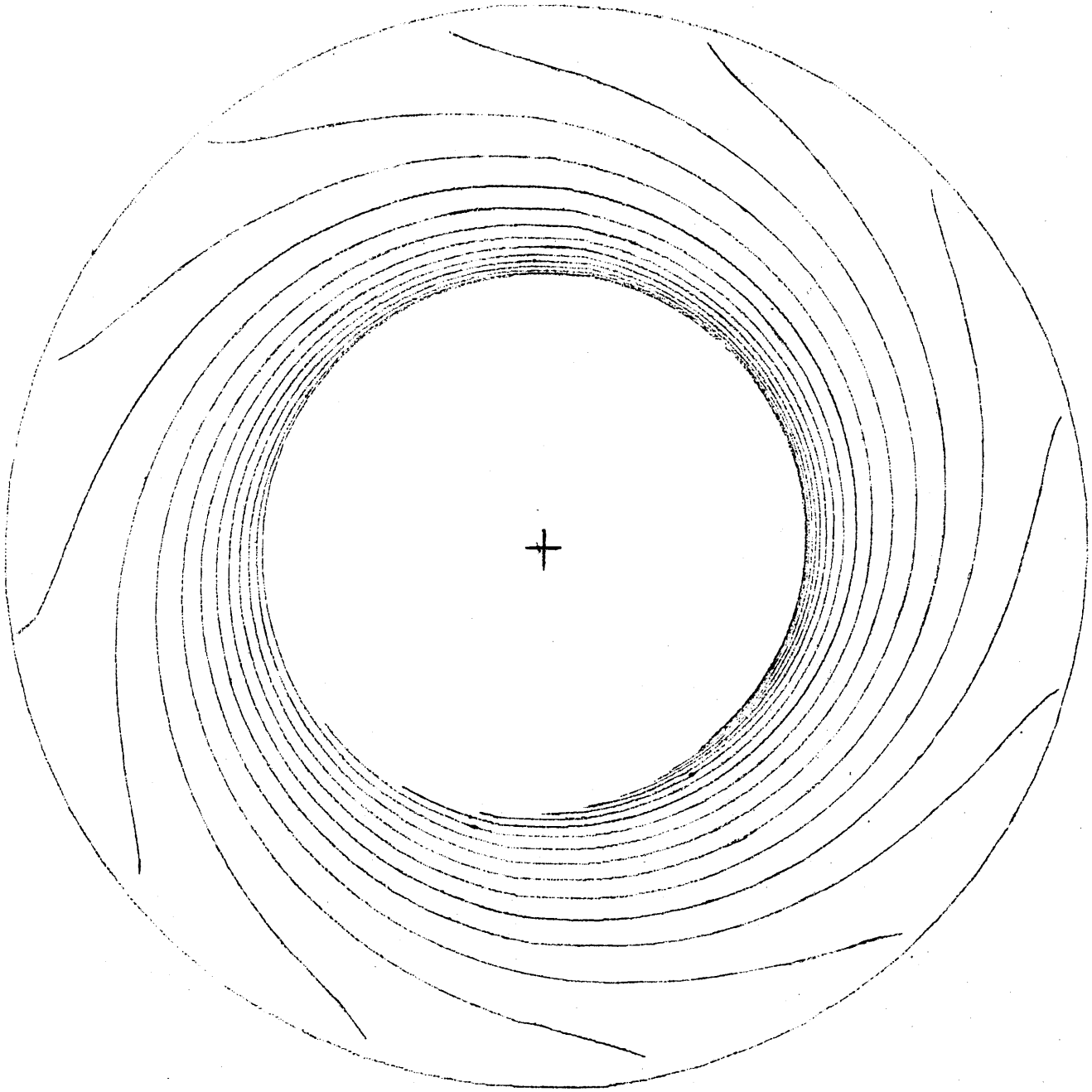

BT= 3.0 WB/M**2

J = 250 KA

N = 0.30E 20 /M**3

F = 805 MHZ

IM= 8 PERCENTS

Fig. 8